

Atmospheric Degradation of 2-Butanol, 2-Methyl-2-butanol, and 2,3-Dimethyl-2-butanol: OH Kinetics and UV Absorption Cross Sections

Elena Jiménez, Beatriz Lanza, Andrés Garzón, Bernabé Ballesteros, and José Albaladejo*

Departamento de Química Física, Facultad de Ciencias Químicas, Universidad de Castilla-La Mancha, Campus Universitario s/n 13071, Ciudad Real, Spain

Received: July 25, 2005; In Final Form: October 11, 2005

The absolute rate coefficients for the reactions of hydroxyl radical (OH) with 2-butanol (k_1), 2-methyl-2-butanol (k_2), and 2,3-dimethyl-2-butanol (k_3) were measured as a function of temperature (263–354 K) and pressure (41–193 Torr of He, Ar, and N₂) by the pulsed laser photolysis/laser-induced fluorescence technique. This work represents the first absolute determination of k_1 – k_3 and their temperature dependence. No pressure dependence of the rate coefficients was observed in the range studied. Thus, k_i (298 K) values ($\times 10^{-12}$ cm³ molecule⁻¹ s⁻¹ with an uncertainty of $\pm 2\sigma$) were averaged over the pressure range studied yielding 8.77 ± 1.46 , 3.64 ± 0.60 , and 9.01 ± 1.00 for 2-butanol (k_1), 2-methyl-2-butanol (k_2), and 2,3-dimethyl-2-butanol (k_3), respectively. k_1 and k_3 exhibit a slightly negative temperature dependence over the temperature range studied. In contrast, the rate coefficient for the reaction of OH with 2-methyl-2-butanol (k_2) did not show any temperature dependence. Some deviation of the conventional Arrhenius behavior was clearly observed for k_3 . In this case, the best fit to our data was found to be described by the three-parameter expression $k(T) = A + B \exp(-C/T)$. The UV absorption cross sections of 2-butanol, 2-methyl-2-butanol, and 2,3-dimethyl-2-butanol have also been measured at room temperature between 208 and 230 nm. The values reported constitute the first determination of the UV cross sections of those alcohols. Our results are compared with previous studies, when possible, and are discussed in terms of the H-abstraction by OH radicals. The atmospheric implications of these reactions and the photochemistry of these alcohols are also discussed.

Introduction

Alcohols are emitted into the atmosphere by different natural and anthropogenic sources. These organic volatile compounds are also produced in the atmosphere from the photooxidation of alkanes initiated by hydroxyl (OH) radicals. Some studies showed that solvent use is the main emission source of these oxygenated hydrocarbons in central Europe.¹ However, emission of 2-butanol by agricultural and natural plant species has also been measured by König et al.² Recently, 2-butanol has been proposed as a candidate for addition to the Clean Air Act list of hazardous air pollutants.³

The atmospheric chemical degradation of alcohols is expected to be their OH-initiated reaction and, to a lesser extent, their reaction with NO₃.⁴ Photolysis of alcohols is expected to be a minor removal process in the troposphere (at wavelengths greater than 290 nm).⁵ Ultraviolet (UV) absorption cross sections of methanol and ethanol have been reported in the wavelength range between 160 and 200 nm.⁵ However, the absorption UV cross sections of longer alcohols such as 2-butanol and its branched derivatives (2-methyl-2-butanol and 2,3-dimethyl-2-butanol) have not been reported yet.

To our knowledge, the kinetic studies on the reaction of OH radicals with 2-butanol (k_1)



were performed exclusively at room temperature and by using only relative methods.^{6,7} Chew and Atkinson used 2-butanol as

a scavenger of the OH radicals formed in the reaction of O₃ with alkenes and monoterpenes.⁶ These authors employed cyclohexanone as a reference compound. On the other hand, Baxley and Wells performed the kinetic study of reaction 1 relative to *n*-nonane and *n*-dodecane.⁷

Up to date no measurements of the rate coefficients of OH with 2-methyl-2-butanol (k_2) and 2,3-dimethyl-2-butanol (k_3) have been reported:



Thus, more kinetic information of the degradation route of these alcohols is needed to fully understand their atmospheric behavior and their impact on the formation of tropospheric ozone. In that sense, we report in this work the gas-phase kinetics of OH radicals with 2-butanol, 2-methyl-2-butanol, and 2,3-dimethyl-2-butanol between 263 and 354 K at total pressures between 41 and 193 Torr of different bath gases (He, Ar, and N₂). We report, herein, the first measurement of the rate coefficients at room temperature k_2 (298 K) and k_3 (298 K) and the first absolute determination of k_1 (298 K). Furthermore, the temperature dependence of the titled reactions is also reported for the first time. The temperature dependence of reactions 1–3 can be used to extrapolate the rate coefficient of these reactions at tropospheric temperatures. The results obtained in this work will extend the kinetic database for these kind of reactions. In this work, we also report the UV absorption cross sections of the mentioned alcohols between 208 and 230 nm at 298 K for the first time.

* Corresponding author. Phone: 34 926 29 53 27. Fax: 34 926 29 53 18. E-mail: Jose.Albaladejo@uclm.es.

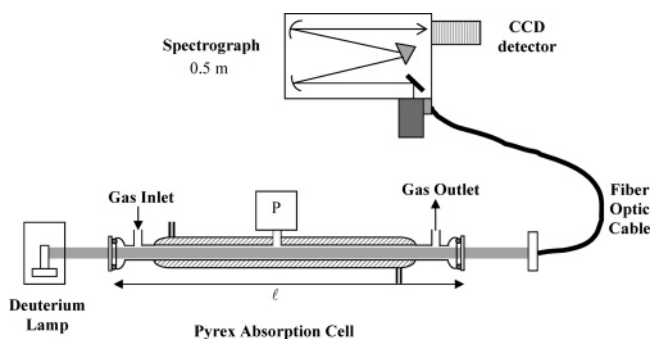


Figure 1. Experimental system employed in the measurements of the absorption cross sections of alcohols.

The description of the two experimental setups employed in this study is given in detail in the Experimental Section. This section is divided in two subsections. The first subsection describes the UV spectroscopy system used to measure the absolute absorption cross sections of the titled alcohols at room temperature. The second one describes the pulsed laser photolysis/laser-induced fluorescence system employed in the OH-kinetic measurements. The Results section has been also divided in two subsections for ease of presentation. The first subsection presents the results obtained for the absolute cross section of the alcohols, and the second one presents the results of the OH kinetic measurements. Finally, our findings will be discussed in terms of the H-atom abstraction. The atmospheric implications of these reactions and the photochemistry of these alcohols will be also discussed.

Experimental Section

UV Absorption Cross-Section (σ_λ) Determination. A newly constructed system was employed to measure the absolute absorption cross sections of 2-butanol, 2-methyl-2-butanol, and 2,3-dimethyl-2-butanol. A scheme is presented in Figure 1.

This system consisted of a jacketed Pyrex cell sealed with quartz windows. A 30-W deuterium lamp irradiated the gas sample, and the transmitted light was focused onto the entrance slit of a 0.5-m spectrometer (Chromex 500is/ms) via a fiber optic cable. Then, the radiation was dispersed by a grating (300 or 1200 grooves/mm with spectral resolutions of 0.19 and 0.04 nm, respectively) and detected by a charge-coupled device, CCD (Andor, 1024×256 pixel²). The detector was cooled to -20 °C using a Peltier cooling system to reduce the dark current during the measurement. Wavelengths were calibrated (± 1.5 nm) using a Hg/Ar pen ray lamp. The optical path length ($\pm 2\sigma$) was ($l = 107.0 \pm 0.2$ cm). The ultraviolet spectrum of these alcohols was recorded between 200 and 350 nm by coadding between 3000 and 5000 spectra to increase the signal-to-noise ratio. All experiments were carried out at room temperature.

The cell was filled with a known pressure of the alcohol (0.2–5 Torr of pure alcohol or 5–100 Torr of a mixture alcohol/carrier gas from a bulb) measured with a 10- or 100-Torr pressure transducer at the center of the UV cell.

OH Kinetic Measurements. A pulsed laser photolysis/laser-induced fluorescence (PLP-LIF) system was employed to measure the rate coefficients k_1 – k_3 as a function of total pressure and temperature. This system has been modified from the one used in other kinetic studies performed by our group on OH radical^{8–10} and other atmospheric radicals^{11,12} to measure the concentration of the OH precursor optically. So, the UV spectroscopy system presented in Figure 1 was coupled to the PLP-LIF system. A brief description of the apparatus is given below.

A Pyrex reactor (internal volume of 200 cm³) was thermostated with methanol, water, or mineral oil circulated through its outer jacket. Reactions 1–3 were studied at several temperatures (263–354 K) and total pressures between 41 and 193 Torr in several bath gases (He, Ar, or N₂). Reactant mixtures were diluted with the carrier gas and stored in a 10-L blackened bulb (0.1–1%). All gases were flowed through the reactor at a total flow rate between 260 and 520 cm³ min⁻¹ (expressed in standard conditions of temperature and pressure). All mass flow meters (carrier gas and H₂O₂/carrier and reactant/carrier gas mixtures) were previously calibrated by measuring the increase of pressure in a known volume at 298 K.

Hydroxyl radicals (OH) were generated by the pulsed UV photolysis of hydrogen peroxide (H₂O₂) at 248 nm using a KrF excimer laser. H₂O₂ was introduced into the reaction cell by bubbling the carrier gas through a H₂O₂ liquid sample at 298 K. The initial OH concentration, [OH]₀, was estimated by using the measured fluence, the absorption cross section of the precursor at 248 nm (σ_λ), the quantum yield for OH production from the precursor at this wavelength ($\phi_{248\text{nm}} = 2$), and concentration of the precursor.¹³ [OH]₀ ranged from 6.4×10^{10} to 1.5×10^{11} molecule cm⁻³. The OH radicals generated in the 248-nm photolysis were excited at ca. 282 nm ($A^2\Sigma^+$, $v' = 1 \leftarrow X^2\Pi$, $v'' = 0$) by using a frequency doubled dye-laser pumped by a Nd:YAG laser. Subsequently, OH radicals were monitored by their laser-induced fluorescence (LIF) near 308 nm. Repetition rate was set to 5 or 10 Hz. LIF signals were detected by a photomultiplier tube and then transferred to a personal computer for further analysis.⁸

Determination of Gas-Phase Concentrations. The concentration of the OH precursor, also involved in the kinetic scheme, was determined by UV spectroscopy prior to entering the reaction cell. Its absorption spectrum was recorded at 298 K between 240 and 290 nm using the same experimental setup employed to measure the absorption cross sections of alcohols. Simultaneously with the OH-kinetic measurement, the H₂O₂ spectrum was recorded using a 1200 grooves/mm grating centered at 260 nm. The H₂O₂ flow ($f_{\text{precursor}}$) was diluted in the reaction cell with the bath gas (f_{bathgas}) and the alcohol (f_{alcohol}) flows. The H₂O₂ concentration in the reaction cell was then calculated by accounting for the differences in pressure and temperature between the absorption and reaction cells. The H₂O₂ concentration was also corrected with the dilution factor. This dilution factor is defined as $f_{\text{precursor}}/f_{\text{total}}$, where f_{total} was the sum of all gas flows entering the reaction cell (H₂O₂, bath gas, and alcohol). The concentration of H₂O₂ was obtained by normalizing the recorded spectrum using the cross sections recommended by the Jet Propulsion Laboratory¹⁴ and the optical path length (the reference spectrum). The residual upon subtraction of the reference spectrum was very small and did not show systematic features. Measured H₂O₂ concentrations in the reaction cell ranged from 5×10^{13} to 1×10^{14} molecule cm⁻³.

Alcohol concentrations were determined from gas flow rates measured using calibrated mass flow meters and the total pressure inside the reaction cell. Reactant concentrations ranged as $(0.10\text{--}4.20) \times 10^{14}$ molecule cm⁻³ for 2-butanol, $(0.21\text{--}6.70) \times 10^{14}$ molecule cm⁻³ for 2-methyl-2-butanol, and $(0.15\text{--}4.60) \times 10^{14}$ molecule cm⁻³ for 2,3-dimethyl-2-butanol.

Reactants. Samples of 2-butanol (99.5%), 2-methyl-2-butanol (99+%), and 2,3-dimethyl-2-butanol (99.5%) were used as supplied after several freeze/pump/thaw cycles. Liquid hydrogen peroxide was concentrated by bubbling helium through an aqueous solution of H₂O₂ (Sharlab, 50% w/v) several days prior use. H₂O₂ concentration in the liquid phase was determined as

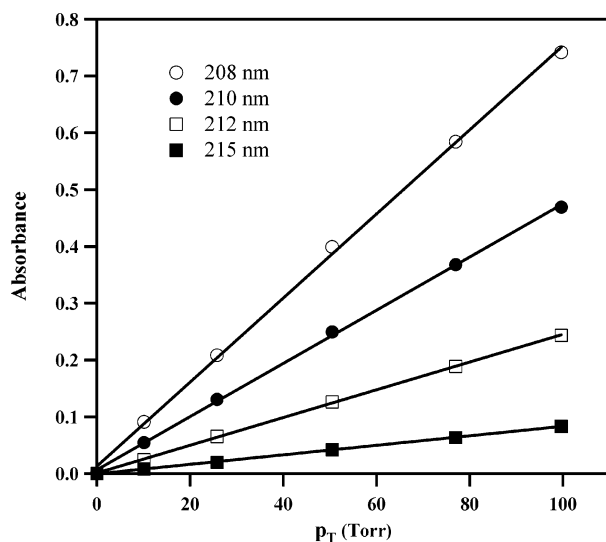


Figure 2. Verification of the Beer–Lambert law for 2-butanol at several wavelengths.

described elsewhere.¹⁰ Carrier gases (99.999%) were used as supplied from Praxair: helium, argon, and nitrogen.

Results and Discussion

UV Absorption Cross-Section Determination. The determination of the absorption cross sections is based on the Beer–Lambert law:

$$A = -\ln\left(\frac{I(\lambda)}{I_0(\lambda)}\right) = \sigma_\lambda lN \quad (\text{I})$$

Here A is the absorbance, σ_λ is the absorption cross section at a wavelength λ , l is the optical path length, and N is the number density in molecule cm^{-3} . $I_0(\lambda)$ and $I(\lambda)$ are the transmitted light intensity measured in the absence and the presence of a known concentration of the alcohol, respectively. Thus, the absolute absorption cross section (base e) at a given wavelength is obtained from the slope of the plot of the natural logarithm of $I(\lambda)$ over $I_0(\lambda)$ versus total pressure in the UV cell (proportional to N). Some examples of these plots are shown in Figure 2 at various wavelengths for 2-butanol. As it can be seen, the Beer–Lambert law is verified over the pressure range used.

An example of the absorption spectrum of 2-butanol between 210 and 350 nm is presented in Figure 3a. However, absolute absorption cross sections were only reported between 208 and 230 nm (see Figure 3b) because (a) the quantum efficiency of the detector is too low at wavelengths shorter than 200 nm to accurately measure σ_λ and (b) the absorption of these alcohols rapidly decreases at wavelengths greater than 200 nm, reaching the baseline around 270 nm (as Figure 3a shows). The maximum absorption of alcohols is presented in the vacuum ultraviolet region.⁵ Thus, we report an upper limit of $1 \times 10^{-21} \text{ cm}^2$ for the absorption cross sections at wavelengths greater than 235 nm (up to 350 nm). These absolute absorption cross sections were determined in several experiments, and the resulting weighted averages of σ_λ are plotted in Figure 3b. As Figure 3 shows, the absorption cross sections of these three alcohols drop off very quickly at $\lambda > 210 \text{ nm}$. Since ozone in the upper atmosphere absorbs most of the radiation at $\lambda < 290 \text{ nm}$, photolysis of alcohols is limited to the spectral region at $\lambda > 290 \text{ nm}$. Thus, in the light of the σ_λ measured, we can conclude that UV–visible photolysis of 2-butanol, 2-methyl-2-butanol,

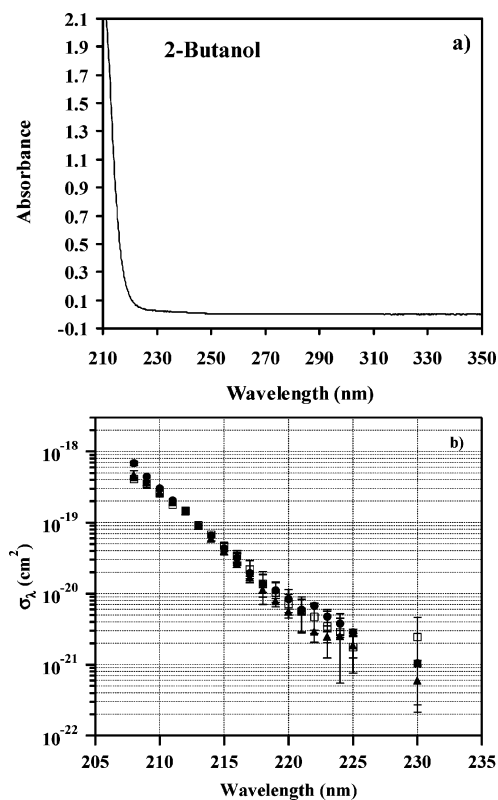
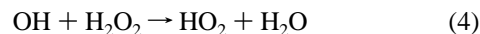


Figure 3. (a) Example of the UV spectrum of 2-butanol (4 Torr) recorded between 208 and 350 nm. (b) Absolute ultraviolet absorption cross sections of alcohols between 208 and 230 nm at room temperature. Key: (□) 2-butanol; (●) 2-methyl-2-butanol; (■) 2,3-dimethyl-2-butanol.

and 2,3-dimethyl-2-butanol is negligible in the actinic region at $\lambda > 290 \text{ nm}$.

OH Kinetic Measurements. The rate coefficient for reactions 1–3 were obtained under pseudo-first-order conditions in the OH radical ($[\text{alcohol}] > 100 [\text{OH}]_0$), over the temperature (263–354 K) and pressure (41–193 Torr) ranges used. In the presence of the alcohol, the OH loss is attributed to reactions 1–3 (k_i), reaction with the precursor, H_2O_2 (k_4), and also diffusion out of the detection zone (k_5):



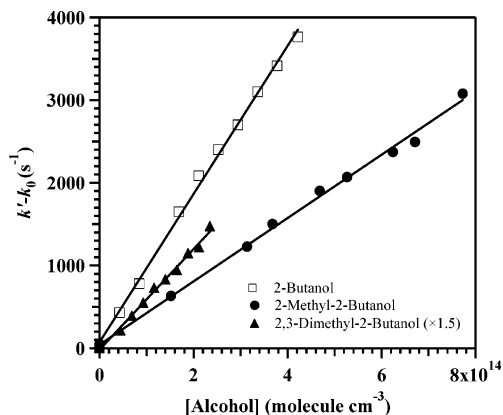
The loss of OH in the absence of reactant is only attributed to reactions 4 and 5. Losses of OH radicals due to its self-reaction are minimized at typical OH initial concentrations ($[\text{OH}]_0 = (0.64\text{--}1.50) \times 10^{11} \text{ molecule cm}^{-3}$). OH temporal profiles followed a simple exponential rate law. The fact that OH temporal profiles (in logarithm scale, i.e., $\ln [\text{OH}]$ versus time) present a very good linearity evidences that the pseudo-first-order conditions are achieved and, thus, the contribution of the OH self-reaction (a second-order reaction) is negligible. The radical decay signal at each reactant concentration was analyzed as described by Albaladejo et al.⁸ to obtain the pseudo-first-order decay rate coefficient (k') due to the reaction under study:

$$k' = k_i[\text{alcohol}] + k_0 \quad (\text{II})$$

$k_0 (=k_4[\text{H}_2\text{O}_2] + k_5)$ is the first-order rate coefficient for the loss of OH in the absence of reactant. The values of k_0 in our measurements ranged from 72 to 1602 s^{-1} . If one knows $[\text{H}_2\text{O}_2]$ and k_4 (from the literature¹⁴), the diffusion rates k_5 obtained

TABLE 1: Comparison of Room-Temperature Rate Coefficients ($\pm 2\sigma$) Obtained in This Work for the Reaction of OH Radicals with 2-Butanol and Two Substituted Derivatives with the Corresponding Alkane

alcohol	$10^{12}k_i(298\text{ K})$ ($\text{cm}^3\text{ molecule}^{-1}\text{ s}^{-1}$)	alkane	$10^{12}k_i(298\text{ K})$ ($\text{cm}^3\text{ molecule}^{-1}\text{ s}^{-1}$)
2-butanol	8.77 ± 1.46	2-methylbutane	3.60^a
2-methyl-2-butanol	3.64 ± 0.60	2,2-dimethylbutane	2.23^a
2,3-dimethyl-2-butanol	9.01 ± 1.00	2,2,3-trimethylbutane	3.81^a

^a Data from Atkinson and Arey.⁴**Figure 4.** Pseudo-first-order plots for the secondary alcohols studied in this work at 298 K.

from the difference $k_0 - k_4[\text{H}_2\text{O}_2]$ ranged as follows: $k_5(\text{He}, \text{Ar}) = 28\text{--}253\text{ s}^{-1}$; $k_5(\text{N}_2) = 60\text{--}723\text{ s}^{-1}$. The minimum reaction decay rate k' in our measurements was 155 s^{-1} whereas the maximum decay rate was 7640 s^{-1} . At each temperature and pressure, the rate coefficient k_i was determined from the slope of a plot of $k' - k_0$ versus alcohol concentration:

$$k' - k_0 = k_i[\text{alcohol}] \quad (\text{III})$$

In Figure 4, an example of these plots at room temperature for 2-butanol, 2-methyl-2-butanol, and 2,3-dimethyl-2-butanol is shown. The values of $k' - k_0$ for the reaction of OH with 2,3-dimethyl-2-butanol have been magnified by a factor of 1.5 for clarity.

Our measured values of k_i were not affected by changes in the residence time of the gas mixture in the reaction cell (linear velocity = $1\text{--}13\text{ cm s}^{-1}$), the bath gas (Ar, He, or N_2), the fluence of the photolysis laser ($1.8\text{--}8.3\text{ mJ pulse}^{-1}\text{ cm}^{-2}$), or the total pressure ($41\text{--}193\text{ Torr}$). These tests indicate a negligible contribution of secondary chemistry involving OH or its precursor and lend confidence to our measured values. Moreover, to check for a possible secondary source of OH radicals, alcohol mixtures were photolyzed at 248 nm using typical laser fluences. Under these experimental conditions, OH radical was not detected, indicating that OH formation in the photolysis of alcohols is negligible at that wavelength. Then, an estimation of the extent of the alcohol loss by photolysis at 248 nm can be made by assuming an upper limit for the quantum yield of 1 and the absorption cross sections of 2-butanol, 2-methyl-2-butanol, and 2,3-dimethyl-2-butanol at 248 nm of $10^{-21}\text{ cm}^2\text{ molecule}^{-1}$. The calculated $[\text{OH}]_0$ from the alcohol photolysis ranged from 2.2×10^7 to $7.0 \times 10^9\text{ molecule cm}^{-3}$. Thus, the alcohol concentration would decrease less than 0.001%, not affecting to the kinetic analysis. So, in practice, OH radicals detected by LIF came exclusively from H_2O_2 photolysis.

Room-Temperature Measurements of k_i . The rate coefficients $k_1\text{--}k_3$ measured at 298 K were independent of total pressure and the bath gas used, in the ranged studied ($41\text{--}193\text{ Torr}$). A

summary of the weighted averages obtained in this work at room temperature is presented in Table 1. The weighted averages of the rate coefficients, according to the precision of the measurement ($w_i = 1/\sigma_i^2$), are (in $\text{cm}^3\text{ molecule}^{-1}\text{ s}^{-1}$) $(8.77 \pm 1.46) \times 10^{-12}$, $(3.64 \pm 0.60) \times 10^{-12}$, and $(9.01 \pm 1.00) \times 10^{-12}$ for 2-butanol, 2-methyl-2-butanol, and 2,3-dimethyl-2-butanol, respectively; the quoted errors are $\pm 2\sigma$. Room-temperature rate coefficients with OH radicals obtained in this work follow this trend:

$$k(2\text{-methyl-2-butanol}) < k(2\text{-butanol}) \approx k(2,3\text{-dimethyl-2-butanol})$$

This trend can be explained in terms of the different types of hydrogen inside the hydrocarbon chain ($-\text{CH}-$, $-\text{CH}_2-$, or $-\text{CH}_3$), since it is known that the reaction of OH with alcohols mainly involves H-atom abstraction from C–H bonds.¹⁵

Our results show that the rate coefficients for the reaction of OH with 2-butanol and 2,3-dimethyl-2-butanol, with one $-\text{CH}-$ group, are very similar and approximately 2.5 times faster than the reaction with 2-methyl-2-butanol, with only one methylene group. Thus, the abstraction of a hydrogen atom attached to a tertiary carbon is faster than that of an H atom from a methylene or methyl group, as expected. These observations are consistent with the rate coefficient reported by Mellouki et al.¹⁶ for the reaction of OH with 3-methyl-2-butanol obtained by a relative method ($(1.25 \pm 0.20) \times 10^{-11}\text{ cm}^3\text{ molecule}^{-1}\text{ s}^{-1}$) and by the PLP-LIF technique ($(1.20 \pm 0.10) \times 10^{-11}\text{ cm}^3\text{ molecule}^{-1}\text{ s}^{-1}$). The reaction of OH with 3-methyl-2-butanol (with two $-\text{CH}-$ groups) is faster than the corresponding reaction with 2,3-dimethyl-2-butanol and 2-butanol (with one $-\text{CH}-$ group).

The effect of the substituent (alcohol or methyl group) on the OH reactivity can also be seen in the comparison of the rate coefficients of the reaction of OH with these alcohols and the corresponding alkanes (see Table 1). The substitution of a CH_3 group by an OH group greatly enhances the reactivity of the resulting alcohol, as expected. In both cases, the OH-reactivities toward alcohols (2-butanol and 2,3-dimethyl-2-butanol) and alkanes (2-methylbutane and 2,2,3-trimethylbutane) containing a $-\text{CH}-$ group are similar. However, the OH-reactivity toward 2-methyl-2-butanol and 2,3-dimethylbutane, with a $-\text{CH}_2-$ group, decreases with respect to those with a $-\text{CH}-$ group, indicating again that OH is more reactive toward an H atom attached to a tertiary carbon than that attached to a secondary carbon.

Table 2 shows a comparison of $k_1(298\text{ K})$ reported here with those found in the literature. Chew and Atkinson⁶ measured the rate coefficient ratio of $k(\text{OH} + 2\text{-butanol})/k(\text{OH} + \text{cyclohexane}) = 1.24 \pm 0.07$ that placed on an absolute basis by using a rate coefficient of $k(\text{OH} + \text{cyclohexane}) = 7.45 \times 10^{-12}\text{ cm}^3\text{ molecule}^{-1}\text{ s}^{-1}$ yielded $(9.20 \pm 2.40) \times 10^{-12}\text{ cm}^3\text{ molecule}^{-1}\text{ s}^{-1}$ at 296 K. In Baxley and Wells' experiments the concentrations of 2-butanol and *n*-nonane and *n*-dodecane (the reference compounds) were measured by gas chromatography. The measured rate coefficient ratios of $k(\text{OH} + 2\text{-butanol})/k(\text{OH} + \textit{n}-nonane) and $k(\text{OH} + 2\text{-butanol})/k(\text{OH} + \textit{n}-dodecane) were$$

TABLE 2: Comparison of Room-Temperature Rate Coefficients Obtained in This Work ($\pm 2\sigma$) for Reaction 1 with Literature Values^a

$k_1(298\text{ K})$ ($10^{-12}\text{ cm}^3\text{ molecule}^{-1}\text{ s}^{-1}$)	technique ^b	ref
8.77 ± 1.46	PLP-LIF	this work
8.10 ± 2.00^c	RR-GC/FID	Baxley and Wells ⁷
9.20 ± 2.40^d	RR-GC/FID	Chew and Atkinson ⁶
8.70^e		Atkinson et al. ¹⁷

^a Uncertainties stated by the authors. ^b RR-GC/FID, relative rate/gas chromatography and flame ionization detection. ^c Relative to *n*-nonane and *n*-dodecane. ^d Relative to cyclohexane. ^e Recommended value in the latest evaluation of the IUPAC subcommittee on gas kinetic data evaluation.

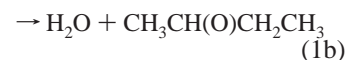
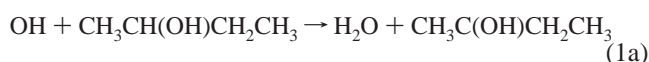
also placed on an absolute basis by using the rate coefficients at 297 K of $k(\text{OH} + n\text{-nonane}) = (1.02 \pm 0.26) \times 10^{-11}\text{ cm}^3\text{ molecule}^{-1}\text{ s}^{-1}$ and $k(\text{OH} + n\text{-dodecane}) = (1.42 \pm 0.36) \times 10^{-11}\text{ cm}^3\text{ molecule}^{-1}\text{ s}^{-1}$.⁷

Within the error limits given, there is a good agreement between our $k_1(298\text{ K})$ and those found by Chew and Atkinson⁶ and Baxley and Wells⁷ using relative techniques. Our value of k_1 is also in very good agreement with the recommended one by the IUPAC evaluation on gas kinetic data.¹⁷ The uncertainty reported in $k_1(298\text{ K})$ in this work has been considerably reduced respect to previous measurements; however, data are still too scattered.

On the basis of the structure–activity relationship (SAR) of Atkinson, OH-rate coefficients (in $\text{cm}^3\text{ molecule}^{-1}\text{ s}^{-1}$) for 2-butanol, 2-methyl-2-butanol, and 2,3-dimethyl-2-butanol were calculated using the AOPWin program from the U.S. EPA¹⁸ obtaining 9.97×10^{-12} , 4.89×10^{-12} , and 8.88×10^{-12} , respectively. As can be seen, while the experimental values of k_1 and k_3 are in good agreement with the calculated ones (within the error limits given), the predicted value of k_2 is a factor of 1.34 higher than the experimental one. Some discrepancy between the experimental and calculated rate coefficients for the reactions of OH with alcohols has already been observed previously. The available rate coefficient data for the OH reaction with alcohols clearly indicate that the OH group has long-range activating effects at sites remote from the substituent group. Wallington et al.¹⁹ and Nelson et al.²⁰ concluded that the activating effects of the OH group in the alcohols extend for several carbon atoms beyond the carbon atom that the OH group is attached to, which is not taken into account in the estimation method of Kwok and Atkinson.²¹

Nelson et al.²⁰ also concluded that the observed long-range activating effect of the OH group cannot be explained in terms of the bond energy or inductive effects, indicating an alternative reaction pathway to the direct concerted H atom abstraction process. Smith and Ravishankara²² have recently discussed the reactions of OH radicals with oxygenated organic compounds in terms of the formation of hydrogen-bonded complexes. Formation of such complexes results in a lower activation energy for the reaction compared with the direct H-atom abstraction reaction. Although this discussion was restricted to carboxylic acids, aldehydes, and ketones, it could be also extended for aliphatic alcohols in a similar manner.

Some mechanistic information is available for the reaction of OH with 2-butanol. However, there are no mechanistic studies on the reactions of OH with 2-methyl-2-butanol and 2,3-dimethyl-2-butanol. The reaction of OH with alcohols can involve H-atom abstraction from several sites; for example, for the OH + 2-butanol reaction, five different channels are possible:



Product studies on the OH + 2-butanol reaction at room temperature indicate that the major reaction channel is the formation of the α -hydroxyalkyl radical (reaction 1a).^{6,7,23,24} Thus, the OH + 2-butanol reaction proceeds mainly by the abstraction from the tertiary C–H bond at room temperature. In the atmosphere, the α -hydroxyalkyl radical reacts with O_2 to form butanone. The measured butanone yield in reaction 1 ranged between $60 \pm 2\%$ ⁷ and $75\text{--}80\%$.²³ Acetaldehyde is also a product of reaction 1. The reported yield of CH_3CHO ranges between 12 and 16% ²³ and 29% .⁷ This product can be formed in reactions 1b,c,e.²³

As far as we know, for the OH-reactions with the branched alcohols studied in this work no product studies have been

TABLE 3: Summary of the Averaged Rate Coefficients Obtained in This Work as a Function of Temperature for the Reaction of OH Radicals with 2-Butanol, 2-Methyl-2-butanol, and 2,3-Dimethyl-2-butanol

$T(\text{K})$	[2-butanol] ($10^{14}\text{ molecule cm}^{-3}$)	$10^{12}(k_1 \pm 2\sigma)$ ($\text{cm}^3\text{ molecule}^{-1}\text{ s}^{-1}$)	[2-methyl-2-butanol] ($10^{14}\text{ molecule cm}^{-3}$)	$10^{12}(k_2 \pm 2\sigma)$ ($\text{cm}^3\text{ molecule}^{-1}\text{ s}^{-1}$)	[2,3-dimethyl-2-butanol] ($10^{14}\text{ molecule cm}^{-3}$)	$10^{12}(k_3 \pm 2\sigma)$ ($\text{cm}^3\text{ molecule}^{-1}\text{ s}^{-1}$)
263	0.19–1.60	9.98 ± 0.30	0.23–3.00	3.91 ± 0.98		
266			0.55–3.30	3.58 ± 0.34		
268	0.20–2.00	9.77 ± 1.46	0.40–2.30	3.39 ± 0.80	0.26–2.60	12.3 ± 1.42
273	0.14–2.00	9.34 ± 0.40			0.25–2.60	11.4 ± 0.22
278	0.25–1.40	8.40 ± 0.40	0.52–2.90	3.89 ± 1.10	0.25–2.30	10.9 ± 0.66
283	0.21–2.30	8.07 ± 0.40	0.20–3.40	3.85 ± 0.80		
288	0.18–1.30	7.90 ± 0.50	0.29–3.70	3.15 ± 0.80	0.29–3.20	9.65 ± 0.76
292					0.13–2.50	9.01 ± 0.90
298	0.10–4.20	8.77 ± 1.46	0.29–6.70	3.64 ± 0.60	0.18–4.60	9.08 ± 1.00
303	0.23–1.50	8.51 ± 2.80	0.34–6.30	3.00 ± 0.60	0.33–2.70	8.39 ± 1.74
313			0.22–5.00	3.94 ± 0.32		
321	0.18–2.10	8.32 ± 1.10	0.33–7.00	2.84 ± 0.98	0.32–2.00	8.30 ± 0.70
327	0.31–5.40	7.93 ± 0.40				
334			0.21–6.20	3.67 ± 0.24		
338	0.18–2.10	6.99 ± 0.48			0.27–2.10	7.34 ± 1.20
343			0.56–6.20	2.78 ± 0.06		
354	0.17–2.50	6.64 ± 0.46	0.28–1.60	3.78 ± 0.52	0.25–1.90	7.51 ± 0.90

reported at room temperature. The effect of the temperature on the product yields of these reactions has not been measured, either. Thus, further studies are needed in that sense.

Temperature Dependence of k_i . The study of the temperature dependence of k_i constitutes the first measurement of the OH kinetics with 2-butanol, 2-methyl-2-butanol, and 2,3-dimethyl-2-butanol as a function of temperature. The temperature was varied between 263 and 354 K. The temperature points for the measurements were chosen to be approximately equally distant along the Arrhenius $1/T$ scale. The weighted averages of $k_1(T)$, $k_2(T)$, and $k_3(T)$ (expressed with an uncertainty of $\pm 2\sigma$) are listed in Table 3, together with the range of alcohol concentration employed in the kinetic measurements. As it can be seen, the rate coefficients for the reaction of OH radicals with 2-butanol and 2,3-dimethyl-2-butanol exhibit a negative temperature dependence (k_1 and k_3 increase when temperature decreases) over the limited temperature range studied. In contrast, the rate coefficient for the reaction of OH radicals with 2-methyl-2-butanol does not show any temperature dependence between 268 and 354 K. This fact can be observed in Figure 5, where Arrhenius plots for $k_1(T)$, $k_2(T)$, and $k_3(T)$ are shown. In addition to the negative temperature dependence of k_1 and k_3 , a slight curvature in the Arrhenius plots was observed (panels a and c in Figure 5). The deviation from the Arrhenius behavior of k_3 is much clearer than that of k_1 and k_2 because of the smaller scattering in the experimental data. A small curvature in the Arrhenius plots of k_1 and k_2 cannot be discarded. For that reason, we consider more appropriate to do an unweighted Arrhenius fit of $k_1(T)$ and $k_2(T)$. The resulting expressions for the rate coefficients of the OH-reaction with 2-butanol and 2-methyl-2-butanol ($\pm 2\sigma$ and expressed in $\text{cm}^3 \text{ molecule}^{-1} \text{ s}^{-1}$) were

$$k_1(T = 263\text{--}354 \text{ K}) = (2.76 \pm 1.20) \times 10^{-12} \exp[(328 \pm 124)/T]$$

$$k_2(T = 263\text{--}354 \text{ K}) = (2.37 \pm 1.70) \times 10^{-12} \exp[(115 \pm 210)/T]$$

As can be seen, the E_a/R factor for the reaction of OH with 2-butanol is slightly negative, while the E_a/R factor is, within the error limits, close to zero for the reaction of OH with 2-methyl-2-butanol; i.e., the rate coefficients of the OH-reaction with 2-methyl-2-butanol are temperature independent in the limited range studied.

Mellouki et al.¹⁶ also found a negative temperature dependence of the rate coefficient for the reaction of OH with 2-methyl-1-propanol ($E_a/R = -(352 \pm 82) \text{ K}$), 3-methyl-1-butanol ($E_a/R = -(503 \pm 98) \text{ K}$), and 3-methyl-2-butanol ($E_a/R = -(456 \pm 65) \text{ K}$). In light of our results and those found in the literature, it seems that the rate coefficients of OH-reaction with alcohols containing a $-\text{CH}-$ group within the hydrocarbon chain exhibit a negative temperature dependence.

For k_3 , where a curvature in the Arrhenius plot is clearly observed, the best fit to our data was found to be described by a three-parameter expression ($k(T) = A + B \exp(-C/T)$). This expression, which has been used by other authors,^{9,25,26} is merely a way to represent the measured values of the rate coefficients, but it is not meant to represent a specific mechanism. Thus, an unweighted three-parameter fit of the rate coefficients for $k_3(T)$ is preferred, resulting in the following expression:

$$k_3(T = 268\text{--}354 \text{ K}) = (5.60 \pm 0.60) \times 10^{-12} + (1.52 \pm 0.21) \times 10^{-14} \exp\{(1620 \pm 268)/T\}$$

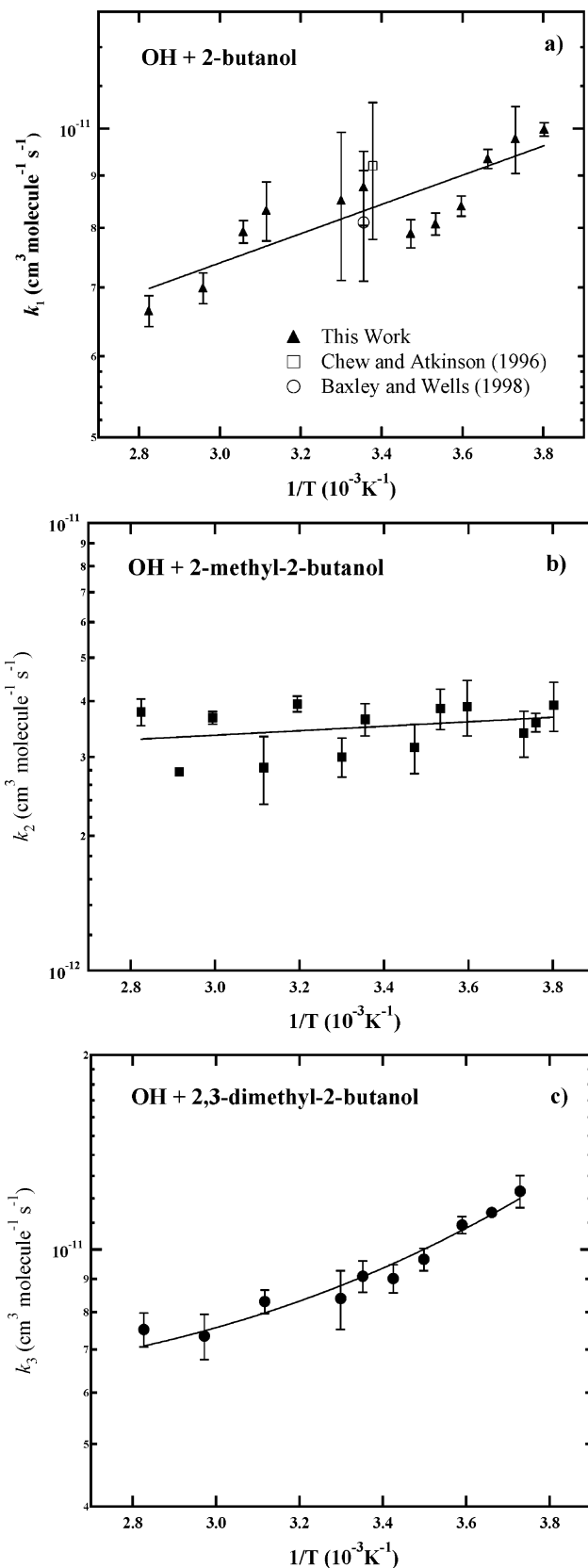


Figure 5. Temperature dependence of k_i over 263 and 354 K: (a) 2-butanol; (b) 2-methyl-2-butanol; (c) 2,3-dimethyl-2-butanol.

The observed pressure independence and the small negative or the absence of a temperature dependence of the rate coefficients, together with some curvature of the Arrhenius plots, suggest that these reactions proceed via a complex rather than a direct mechanism with different reaction pathways for the

H-atom abstraction, including the direct abstraction and the possible formation of hydrogen-bonded adducts. Further product studies are needed to clarify the relative contribution of the different pathways in each of these reactions.

Tropospheric Implications. The results of the kinetic studies presented in this work indicate that alcohols undergo attack by OH radical. The photooxidation of alcohols initiated by NO₃ radical can be important at night, but it is a minor removal process for alcohols since the rate coefficients are 3 orders of magnitude lower than those for OH radicals.⁴ O₃ reactions with alcohols are not expected. Furthermore, as we discussed previously, the photodissociation of alcohols in the actinic region seems to be negligible. Thus, the tropospheric persistence (in parentheses) of 2-butanol (1.3 days), 2-methyl-2-butanol (3.2 days), and 2,3-dimethyl-2-butanol (1.3 days) is due to the chemical removal by OH reaction. That was calculated ($\tau_{\text{OH}} = 1/k_{\text{OH}}$) using an averaged OH concentration of 1.0×10^6 molecule cm⁻³.²⁷ While reaction with hydroxyl radical is the major chemical removal process for alcohols in the atmosphere, physical removal, such as dry and wet deposition, should be taken into account. Thus, those atmospheric lifetimes would be an upper limit for these alcohols.

Acknowledgment. The authors thank the Spanish Ministerio de Ciencia y Tecnología (Grant CGL2004-03355/CLI) and the Junta de Comunidades de Castilla-La Mancha (Project No. PAI-05-062) for supporting this project.

Supporting Information Available: Table showing absolute absorption cross sections. This material is available free of charge via the Internet at <http://pubs.acs.org>.

References and Notes

- (1) Becker, K. H.; Kurtenbach, R.; Niedojadlo, A.; Wiesen, P. Measurements of oxygenated VOC emissions in the city of Wuppertal, Germany, and in the Plabutsch tunnel, Austria; 7th EUROTRAC Symposium, Garmisch-Partenkirchen, Germany, March 11–15, 2002, Margraf Verlag.
- (2) König, G.; Brunda, M.; Puxbaum, H.; Hewitt, C. N.; Duckham, S. C.; Rudolph, J. *Atmos. Environ.* **1995**, *29*, 861–874.
- (3) Lunder, S.; Woodruff, T. J.; Axelrad, D. A. *J. Air Waste Manag. Assoc.* **2004**, *54*, 157–171.

- (4) Atkinson, R.; Arey, J. *Chem. Rev.* **2003**, *103*, 4605–4638.
- (5) Calvert, J. G.; Pitts, J. N. *Photochemistry*; John Wiley: New York, 1966.
- (6) Chew, A. A.; Atkinson, R. *J. Geophys. Res., Atmos.* **1996**, *101*, 28649–28653.
- (7) Baxley, J. S.; Wells, J. R. *Int. J. Chem. Kinet.* **1998**, *30*, 745–752.
- (8) Albaladejo, J.; Ballesteros, B.; Jimenez, E.; Martin, P.; Martinez, E. *Atmos. Environ.* **2002**, *36*, 3231–3239.
- (9) Jimenez, E.; Ballesteros, B.; Martinez, E.; Albaladejo, J. *Environ. Sci. Technol.* **2005**, *39*, 814–820.
- (10) Albaladejo, J.; Ballesteros, B.; Jimenez, E.; de Mera, Y. D.; Martinez, E. *Atmos. Environ.* **2003**, *37*, 2919–2926.
- (11) Martinez, E.; Albaladejo, J.; Jimenez, E.; Notario, A.; Aranda, A. *Chem. Phys. Lett.* **1999**, *308*, 37–44.
- (12) Albaladejo, J.; Jimenez, E.; Notario, A.; Cabanas, B.; Martinez, E. *J. Phys. Chem. A* **2002**, *106*, 2512–2519.
- (13) Jimenez, E.; Gilles, M. K.; Ravishankara, A. R. *J. Photochem. Photobiol., A* **2003**, *157*, 237–245.
- (14) Sander, S. P.; Friedl, R. R.; Golden, D. M.; Kurylo, M. J.; Huie, R. E.; Orkin, V. L.; Moortgat, G. K.; Ravishankara, A. R.; Kolb, C. E.; Molina, M. J.; Finlayson-Pitts, B. J. *Chemical Kinetics and Photochemical Data for Use in Atmospheric Studies. Evaluation Number 14*; Jet Propulsion Laboratory, California Institute of Technology: Pasadena, CA, 2003; Vol. 02-25.
- (15) Grosjean, D. *J. Braz. Chem. Soc.* **1997**, *8*, 433–442.
- (16) Mellouki, A.; Oussar, F.; Lun, X.; Chakir, A. *Phys. Chem. Chem. Phys.* **2004**, *6*, 2951–2955.
- (17) Atkinson, R.; Baulch, D. L.; Cox, R. A.; Crowley, J. N.; Hampson, R. F. J.; Hynes, R. G.; Jenkin, M. E.; Kerr, J. A.; Rossi, M. J.; Troe, J. *Summary of Evaluated Kinetic and Photochemical Data for Atmospheric Chemistry*; IUPAC: Oxford, U.K., 2005.
- (18) Meylan, W. M.; Howard, P. H. *Chemosphere* **1993**, *26*, 2293–2299.
- (19) Wallington, T. J.; Skewes, L. M.; Siegl, W. O.; Wu, C. H.; Japar, S. M. *Int. J. Chem. Kinet.* **1988**, *20*, 867–875.
- (20) Nelson, L.; Rattigan, O.; Neavyn, R.; Sidebottom, H.; Treacy, J.; Nielsen, O. *Int. J. Chem. Kinet.* **1990**, *22*, 1111–1126.
- (21) Kwok, E. S. C.; Atkinson, R. *Atmos. Environ.* **1995**, *29*, 1685–1695.
- (22) Smith, I. W. M.; Ravishankara, A. R. *J. Phys. Chem. A* **2002**, *106*, 4798–4807.
- (23) Carter, W. P. L.; Darnall, K. R.; Graham, R. A.; Winer, A. M.; Pitts, J. N. *J. Phys. Chem.* **1979**, *83*, 2305–2311.
- (24) Aschmann, S. M.; Arey, J.; Atkinson, R. *Atmos. Environ.* **2002**, *36*, 4347–4355.
- (25) Gierczak, T.; Gilles, M. K.; Bauerle, S.; Ravishankara, A. R. *J. Phys. Chem. A* **2003**, *107*, 5014–5020.
- (26) Dlugokencky, E. J.; Howard, C. J. *J. Phys. Chem.* **1989**, *93*, 1091–1096.
- (27) Dorn, H. P.; Brandenburger, U.; Brauers, T.; Hausmann, M.; Ehhalt, D. H. *Geophys. Res. Lett.* **1996**, *23*, 2537–2540.